

## Experimental and analytical study on liquefied sand behavior under an embankment with PFS method

K. Fujiwara

Lecturer, Tokai University, Department of Civil Engineering, Hiratsuka prefecture, Japan

### ABSTRACT

Steel walls were installed at the toe of an embankment on loose and saturated sand to reduce the embankment settlement caused by liquefaction. Specifically, the partially floating sheet pile (PFS) method uses a steel wall structure consisting of partially floating and end-bearing sheet piles for embankment reinforcement. Although this structure has gaps between the floating-sheet piles, the behavior of the liquefied sand in the gaps is crucial for applying this structure to coastal embankments. However, the behavior of liquefied sand near underground walls remains unclear. In this study, several experiments were conducted to confirm the behavior of liquefied sand near and between underground structures. Six experimental tests were conducted by changing the size of the gaps between the structures and the duration of the earthquake. These experiments allowed the displacement and direction of movement of liquefied sand near underground structures to be determined for each condition during an earthquake. The relationships between embankment settlement and conditions (gap size and earthquake duration) were also quantified. For example, the larger the gap, the greater the displacement of the liquefied sand and, thus, the greater the embankment settlement. Additionally, the author proposed a 2D numerical analysis model to estimate the embankment settlement of 3D underground structures with gaps between walls in different embankment weight and earthquake durations.

*Key words: PFS method, Earthquake, Liquefaction, Experimental test, Numerical analysis*

### 1. Outline of the project

Loose sand layers along river embankments are continuously damaged and settled by liquefaction caused by earthquakes. As a conventional countermeasure, sheet piles are installed at both toes of the embankment to prevent damage and settlement along the embankment, as shown in **Fig. 1(a)** (Fujiwara et al, 2017).

Currently, the partially floating sheet-pile (PFS) method, which uses a steel wall structure consisting of partially floating sheet-piles and end-bearing sheet-piles, is proposed as a river embankment countermeasure against soil settlement due to consolidation, as shown in **Figs. 1(b) and 2**. In the case of the 2016 Kumamoto earthquake, according to a field survey, the damage caused by both consolidation and liquefaction was suppressed near the river embankment, where the PFS

method was applied (Otani, 2017). Although the PFS was originally developed as an anti-consolidation countermeasure, it may also be effective as an anti-liquefaction countermeasure when combined with another side of the sheet pile, as shown in **Fig. 1(c)**.

Therefore, the author conducted experimental model tests and numerical analyses (FEM) to confirm the effectiveness of PFS against liquefaction. Based on this discussion, the following conclusions were drawn (Fujiwara, 2023):

- 1) Based on the experimental model tests, the larger the gap between the floating sheet piles, the larger the horizontal displacement of the liquefied sand in the gap and the larger the embankment settlement.
- 2) Through two-dimensional numerical analyses, the experimental results for the same length of all sheet piles

or no sheet piles were almost well reproduced. This is because these structures have the same cross-section along the depth direction of the embankment, which is called a two-dimensional structure.

3) The PFS does not have the same cross-section, which is called a three-dimensional structure. However, an appropriate method was proposed in which the experimental test results of the PFS could be estimated from the analytical two-dimensional results.

However, these experimental model tests and numerical analyses were conducted under specific conditions (e.g., soil, walls, and earthquake motion). In this study, the author conducted experimental model tests and two-dimensional numerical analyses using twice the duration of the earthquake to more generalize the above conclusions 1–3.

## 2. Experimental study

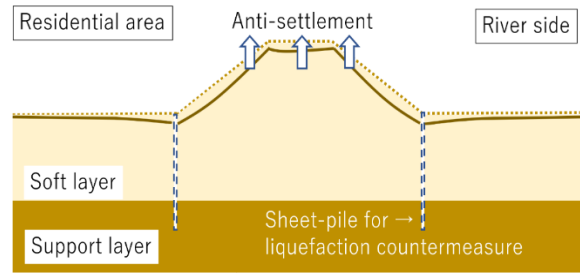
### 2.1. Test condition

Eighteen experimental tests were conducted to study the behavior of liquefied sand in the gap and the embankment settlement by varying the size of the gaps between the walls and the duration of the earthquake.

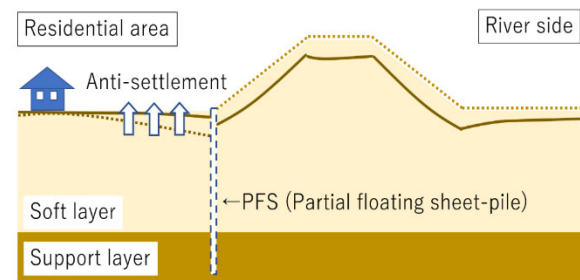
### 2.2. Device

A shaking platform (755 × 365 mm) with a hydraulic vibration generator was used for the model tests. A rigid stainless steel box was used for the experiments, as shown in Fig. 3. The scale of the model embankment was approximately 1/25 the actual size. The values in the model test were converted to correspond to the actual size by using the 1-g similarity rule (Iai, 1988). The permeability coefficient and input motion in the experimental test were significantly greater than those calculated from the actual conditions based on the similarity rule. Therefore, there is no discussion on the comparison between the model and actual sizes in this study.

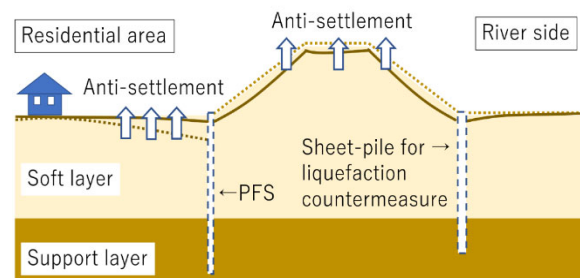
A half embankment was used for the experimental tests. The box is 355 mm wide, 170 mm high, and 200 mm deep. The box interior was separated into two plates. These plates were modeled as sheet piles in the model tests. Two stainless-steel plates were placed 300 mm from the edge of the box. The plates were 170 mm high and 5 mm thick; therefore, they could be considered rigid.



(a) Sheet-piles as liquefaction countermeasures



(b) PFS used to prevent settlement by consolidation



(c) Hybrid countermeasure

**Fig. 1** Countermeasures for the river embankment

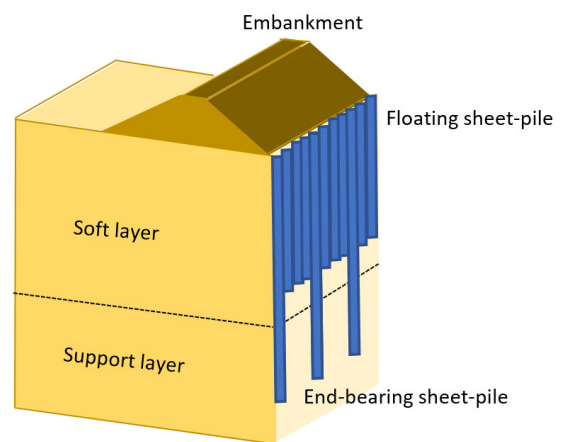


**Fig. 2** The PFS method

The tops and bottoms of the plates were attached to a rigid box with bolts. Six gap sizes were created by using different plate widths.

### 2.3. Cases

Eighteen model tests were conducted, as listed in Table 1. Two different vibration durations (7 s or 11 s) and two different weights (single or double) were used for each case. A gap size of 200 mm indicated that no plate was used, that is, no sheet pile. A gap size of 0 mm indicated that there was no gap; that is, there were all end-bearing sheet piles. These cases can be called “2D” because these structures have the same cross section along the depth. Conversely, test cases with a gap size of 20 mm to 90 mm can be called “3D” because they do not have the same cross section along the depth. These dimensions are discussed in the following sections.

### 2.4. Measurements

The plain and cross-sections are shown in Fig. 3. Two displacement sensors, designated as D1 and D2 in Fig. 3, were used to measure weight settlement. Two excess pore water pressure sensors, designated P1 and P2 in Fig. 3, were used to confirm liquefaction.

### 2.5. Materials

Water and Toyoura sand were added to the box up to a thickness of 170 mm. Toyoura sand with a soil density of  $\rho_s = 2.64 \text{ g/cm}^3$ , maximum void ratio  $e_{\max} = 0.927$ , minimum void ratio  $e_{\min} = 0.635$ , permeability coefficient  $k = 1.94 \times 10^{-2} \text{ cm/s}$ , uniformity coefficient  $U_c = 1.37$ , and 50% diameter  $D_{50} = 0.325 \text{ mm}$  was used as the liquefiable sand. A saturated sand layer with a saturated weight per unit volume ( $\gamma_{\text{sat}}$ ) of approximately  $18.7 \text{ kN/m}^3$  and a relative density ( $D_r$ ) of approximately 45% was used for the experimental tests. A stainless steel weight was placed on one side of the soil surface. The size of the weight was  $141 \text{ mm} \times 195 \text{ mm} \times 14 \text{ mm}$ . The 3 kg weight simulates the load of a typical embankment for this model's scale. There were gaps of about 2 mm between the weight and side walls of the box. As the right side of the weight (Fig. 3) was not connected to the side of the box, the experimental conditions were not strictly symmetrical.

**Table 1.** Test cases

Cases	Duration (seconds)	Gap size (mm)	Weight	Dimension
1-1	7	200	Single	2D
1-2		0		
1-3		20		3D
1-4		50		
1-5		70		
1-6		90		
2-1		7		
2-2	0			
2-3	20		3D	
2-4	50			
2-5	70			
2-6	90			
3-1	11			200
3-2		0		
3-3		20	3D	
3-4		50		
3-5		70		
3-6		90		

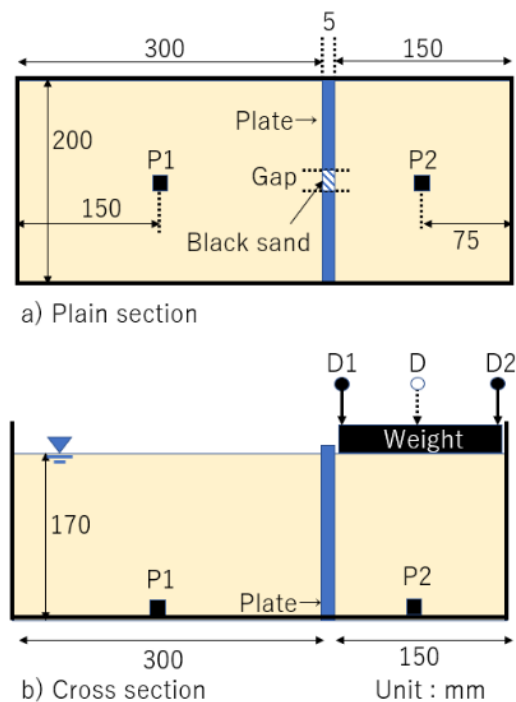


**Fig. 3** Model test

### 2.6. Vibration

A vibration, a sine wave with a frequency of 3 Hz, a duration of 7 or 11 s, and a maximum amplitude of  $2 \text{ m/s}^2$  was applied to the basement.

## 2.7. Test results

### 2.7.1 Representative case (Case 3-1)

The behavior and damage in this model test are explained using Case 3-1 as a representative case. There were no plates in Case 3-1. The time histories of the excess pore water pressure ratio for P1 and P2 are shown in Fig. 4. The excess pore water pressure ratio is a value that the excess pore water pressure is divided by the initial effective vertical stresses (effective weight per unit volume  $\times$  depth). The excess pore water pressure ratio at P1(Case 3-1) reached 1.0, that is, the sand liquefied around P1(Case 3-1). The initial effective vertical stress at P2(Cases 2-1 and 3-1) was greater than that at P1(Case 3-1), owing to its weight. Therefore, the excess pore water pressure ratio at P2(Cases 2-1 and 3-1) did not reach 1.0, indicating that the sand did not liquefy around P2(Cases 2-1 and 3-1). After vibration, the excess pore water drained out from the surface, and the water pressure dissipated within 25 s. The time histories of the settlement displacement at D are shown in Fig. 5. The settlement at D was calculated from the average displacements at D1 and D2. The residual settlements were 73 mm, 88 mm, and 80 mm at D1, D2, and D, respectively.

### 2.7.2 All cases

The relationship between the gap size and residual settlement for all cases is shown in Fig. 6.

For Cases 1-1–1-6, as the gap size decreased, the settlement decreased. As the plate prevented the liquefied sand from moving toward the outside (in the left direction in Fig. 3), the weight settlement was reduced. For Case 1-2, the settlement was reduced by 95% compared to Case 1-1 at D. For Cases 1-3–1-6, as the liquefied sand passed through a gap, it caused settlement in accordance with their gap sizes. These results indicate that installing a wall at the toe of an embankment is effective against settlement, even when there is a gap.

For Cases 1-x and 2-x ( $x = 1-6$ ), there was a difference between single and double weights. The settlement in Case 2-1 was smaller than that in Case 1-1. This is because the vertical stress for Case 2-1 was larger than that for Case 1-1, and the generation of excess pore water pressure was suppressed in Case 2-1 at P2, as indicated in Fig. 4. The initial settlements for Cases 1-1

2-1, and 3-1 were 2, 5 and 2 mm, respectively. However, the initial settlements were omitted from the discussion on soil structure damage and the effectiveness of countermeasures against earthquakes.

For Cases 1-x and 3-x ( $x = 1-6$ ), there was a difference in the duration of 7 and 11 s, respectively. The settlement in Case 3-x was larger than that in Case 1-x. Naturally, the longer the duration, the larger the settlement.

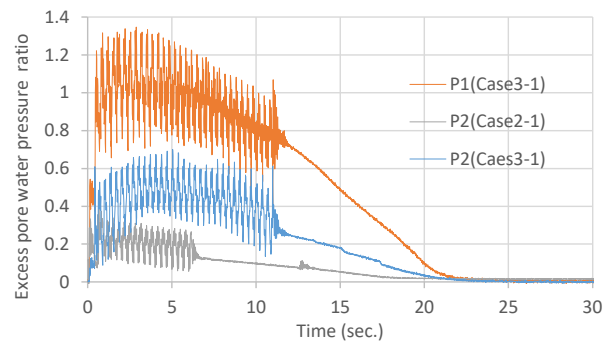


Fig. 4 Time histories of the excess pore water pressure ratio at P1 (Case 3-1), P2 (Case 2-1), and P2 (Case 3-1)

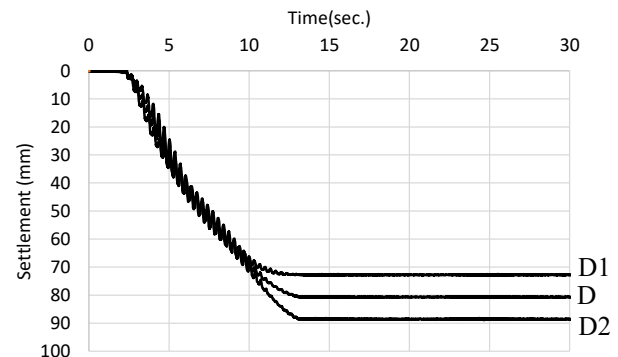


Fig. 5 Time histories of settlement at D1, D2, and D for Case 3-1

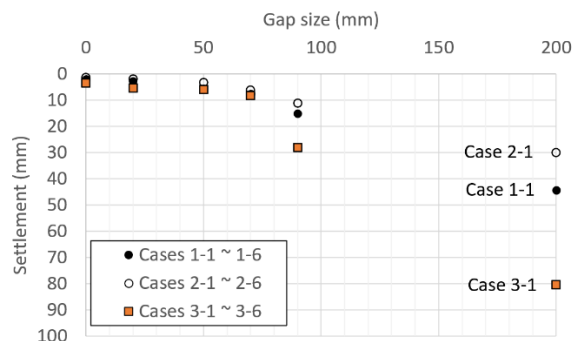


Fig. 6 Relationship between gap size and residual settlement for all cases

### 3. Numerical analysis

#### 3.1. Outline

Numerical analyses of the underground structures with gaps were performed using LIQCA2D20 (LIQCARI, 2020). LIQCA has been used in numerical analyses of the behaviors of embankments, retaining walls, and buildings, as well as in other structures under the liquefaction of the foundation.

#### 3.2. Numerical model condition

Reproducibility analyses were conducted to confirm the accuracy of the numerical analyses for Cases 1-1, 1-2, 2-1, 2-2, 3-1, and 3-2. As these cases were 2D structures, 2D numerical modeling was performed, as shown in Fig. 7. The target underground structure in the numerical model was a plane field. Vertical loads equivalent to the weight was uniformly applied to the nodes on the ground surface. The sand and plates in the box were divided using a multisquare mesh. The locations of the target points D, P1, and P2 in Fig. 7 were identical to the experimental conditions. Meshes from  $x = 300$  mm to  $x = 305$  mm were applied using sand material for Cases 1-1, 2-1, and 3-1 and with plate material for Cases 1-2, 2-2, and 3-2, respectively.

The plates were installed along the x direction at  $x = 300$  mm. The plate was modeled using cubic meshes with a Young's rigidity of  $2.0 \times 10^8$  kN/m<sup>2</sup> and a thickness of 5 mm. Joint elements were placed between the sides of the plate and surrounding sand to account for friction and slip. The joint spring stiffness in the shear and perpendicular directions of the joint elements was set to  $3.3 \times 10^4$  kN/m<sup>2</sup> and  $2.0 \times 10^8$  kN/m<sup>2</sup>, respectively. The soil was modeled as a cyclic elastoplastic model (Oka et al., 1994 and 1999), as shown in Table 2. An incremental time interval of 0.001 s was used, while a value of 0.3025 was used for the coefficient  $\beta$  in the Newmark method, and the value of  $\gamma$  was set at 0.6. We used a stiffness-proportional coefficient of 0.0018 for the Rayleigh damping.

#### 3.3. Numerical result

For Cases 3-1 and 3-2, the deformations with excess pore water pressure ratios corresponding to the end of the vibration ( $t = 10$  s) are represented by the contour plots shown in Fig. 8. The excess pore water pressure ratio is

obtained by dividing the excess pore water pressure by the initial effective stress. The sand under the weight

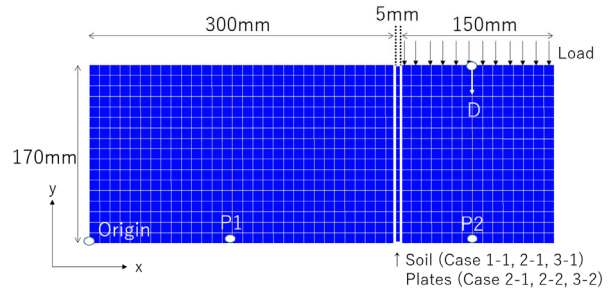


Fig. 7 Numerical model

Table 2. Soil parameters

Initial stress analysis		Unit	Value
Density	$\rho$	t/m <sup>3</sup>	1.91
Young's modulus	$E_0$	kN/m <sup>2</sup>	1210
Poisson's ratio	$\nu$		0.33
Cohesion	$C$	kN/m <sup>2</sup>	0
Friction angle	$\phi$	degree	42
Dynamic analysis			
Coefficient of permeability	$k$	m/s	$2.0 \times 10^{-4}$
Initial void ratio	$e_0$		0.856
Compression index	$\lambda$		0.018
Swelling index	$\kappa$		0.0055
	OCR*		1
Initial elastic shear modulus ratio	$G_0/\sigma'_m$		873
Stress ratio at critical state	$M^*_m$		0.909
Stress ratio at failure	$M^*_f$		1.122
	$B^*_0$		2200
Hardening parameter	$B^*_1$		30
	$C_f$		2000
	$D_0$		5
Dilancy parameter	$n$		1.5
	$\gamma^{p*}$		0.005
Reference strain parameter	$\gamma^{E*}$		0.01

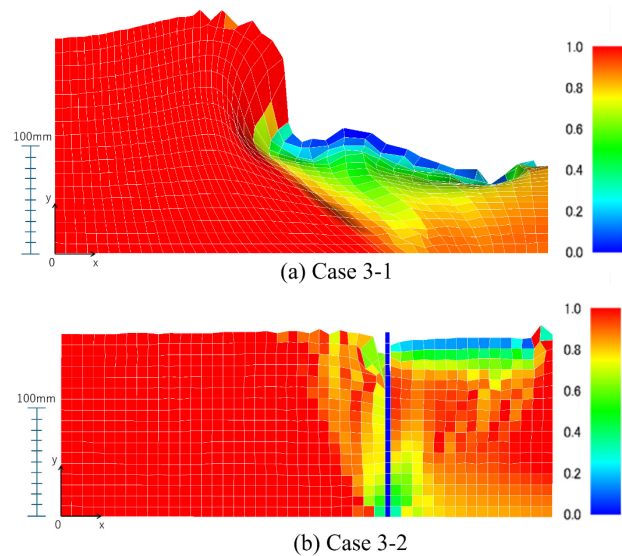
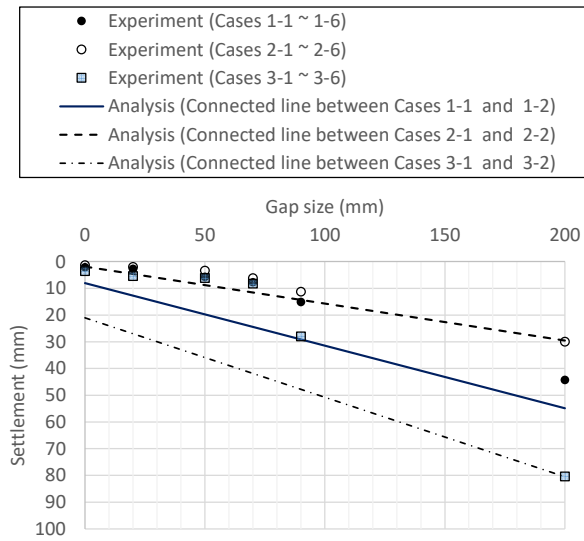


Fig. 8 Deformations with excess pore water pressure ratio ( $t = 10$  s)



**Fig. 9** Residual settlements for the experiments and analyses

(ranging from  $x = 305$  to  $x = 455$  mm) was settled by the vertical load. Although the increase in the excess pore water pressure ratio was relatively small for the sand under weight, the ground without a vertical load (which ranged from  $x = 0$  mm to  $x = 300$  m) reached the point of liquefaction. The sand flowed laterally to the left, as shown in Case 3-1, because of the vertical load during liquefaction, which caused the weight to settle. In Case 3-2, sand was prevented from flowing through the plates; therefore, the settlement was very small, as indicated by the experimental test results. The same behavior was observed for Cases 1-1, 1-2, 2-1, and 2-2.

The residual settlements at D in the numerical analyses and experimental tests are shown in **Fig. 9**. Here, the settlements in the numerical analyses are the average values of surface settlements ranging from  $x = 305$  to  $x = 455$  mm. This is because the analytical results show that the surface of the ground is undulating in **Fig. 8**. In this analysis model, the method of applying vertical loads should be improved in the future.

The solid and dotted lines indicate the numerical analyses connecting the two cases (Cases  $x-1$  and  $x-2$  ( $x = 1, 2, 3$ )). The experimental settlements for almost all cases were estimated using numerical analyses on the safety side. Therefore, even 3D structures such as Cases  $x-3-x-6$  ( $x=1, 2, 3$ ) can be estimated based on the 2D structure results. Although the linear lines calculated from a 2D numerical model were used here for simplicity,

a 3D numerical model was originally required for Cases 1-3 ~ 1-6, Cases 2-3 ~ 2-6 and Cases 3-3 ~ 3-6. Further discussion is needed for setting up such lines.

#### 4. Concluding remarks

Experimental tests and 2D numerical analyses were performed against the embankment installed by walls with gaps. Eighteen experimental tests were performed to confirm the relationship between the size of the gap and the embankment settlement due to liquefaction. 2D numerical analyses were performed to confirm the reproducibility of the experimental results and to propose a 2D analysis method for 3D underground structure. As a result, even 3D structures, which have a wall with a gap, could be estimated based on 2D structure analytical results for the conditions of different earthquake durations and embankment weight.

#### References

- Fujiwara, K, 2017. Reinforcement method for coastal dyke using double sheet-pile against large earthquake, *Doctoral thesis of Gifu University* (in Japanese).
- Fujiwara, K, 2023. Experimental Study on Liquefied Sand Behavior under an Embankment with Walls, *Proceedings of the Annual International Offshore and Polar Engineering Conference*, pp. 1259 - 1266
- Otani, J, 2017. A new sheet-pile method for countermeasures against the settlement of embankment on soft ground (Development of PFS Method), *IPA News Letter*, Vol. 2, Issue 3, pp.8-10.
- Iai, S, 1988. Similitude for Shaking Table Test on Soil structure-Fulid Model in 1 g Gravitation Field, *Report Port Harbor Res Inst*, 27(3), pp. 3-24.
- LIQCARI 2020. LIQCA2D20-3D20, *LIQCA Liquefaction Geo research Institute*.
- Oka, F, Yashima, A, Shibata, T, Kato, M, and Uzuoka, R, 1994. FEM-FDM Coupled Liquefaction Analysis of a Porous Soil Using an Elastic-Plastic Model, *Appl Sci Res*, 52, pp. 209-245.
- Oka, F, Yashima, A, Tateishi, A, Taguchi, Y, and Yamashita, A, 1999. A Cyclic Elasto-Plastic Constitutive Model for Sand Considering a Plastic-Strain Dependence of the Shear Modulus, *Geotechnique*, 49(5), pp. 661-680.